

Fault seal analysis in 'branched' fault traps, eastern Gippsland Basin

Jacques Sayers

Central Petroleum Pty Ltd
 PO Box 197, South Perth WA 6951
 jacquessayers@centralpetroleum.com.au

SUMMARY

The impact of small-scale and 'branched' faults in the assessment of fault-trap integrity often remains unknown or unresolved when risking/evaluating a lead or prospect in regards to its petroleum prospectivity. The following study considered 40 leads in the eastern Gippsland Basin and assessed the overall impact of branch lines on fault trap integrity.

Faults and surfaces were interpreted within a 30X50 km area using a 3-D seismic volume, depth-converted using purpose-programmed software and, a fault seal analysis carried out on the top three ranked leads. The fault seal analysis was underpinned by logs from 13 wells located in and adjacent to the leads.

It was found that the likelihood of fault reactivation increased for 32% of the branch-line cases considered, reduced for 26% of cases while the change being minimal for the remaining 42%. Overall, modelling of the volume of shale attribute indicated that it is unlikely that sand-on-shale windows can be maintained along fault-strike lengths that range up to 20 km.

The study conclusively demonstrates that the primary factor affecting fault-trap integrity in the Halibut Subgroup is the high proportion of across-fault sand-on-sand windows; by comparison, the contribution of fault tips, 'branched' faults and presence of shale smear is secondary. One implication is that the fault-trap integrity for leads located in the eastern Gippsland Basin is more likely to be enhanced closer to the depocentre where the shale content is anticipated to be higher.

Key words: fault seal analysis, fault trap, 3-D seismic interpretation, Gippsland Basin.

INTRODUCTION

Numerous faults exist in the eastern Gippsland Basin so that plays are, in part, contingent on petroleum migration and drainage cells being relatively unimpeded by fault baffling. Early 2-D -based fault interpretations (Maung, 1992) became superseded by 3-D -based fault interpretations (Power *et al.*, 2003), the latter demonstrating increased complexity in the form of relay structures and ramps. In addition, rotation of the principle stress directions was deduced from the varying fault-trend azimuths resulting from rifting in the Cenomanian (~ 95 Ma) to plate-collision involving deformation and reactivation in the Late Miocene (~ 10 Ma). While the role of intraplate stress on trap formation in the Late Miocene is well recognised (Etheridge *et al.*, 1991), the present-day state-of-stress in southeast Australia was firmed up following borehole interpretations of the maximum (S_{Hmax}), minimum (S_{Hmin}) and vertical (S_v) principle stresses (Nelson *et al.*, 2006).

Principal stresses are required for fault reactivation modelling. To date, fault reactivation modelling of isolated 2-D regionally-based interpretations indicate that NW-SE-trending faults had a high likelihood of reactivation in the case of increased pore pressure resulting from CO₂ injection (van Ruth *et al.*, 2006). In the case of estimating trap integrity for petroleum prospects or leads, a comprehensive fault seal analysis is best obtained when using a 3-D volume where a greater number of faults can be interpreted. Breach-of-trap is often associated where multiple faults are involved, often when these have a common branch line (i.e. 'branched'). Ideally, across-fault juxtaposition and fault damage must be incorporated in the fault seal analysis.

The methodology and results below provide a comprehensive assessment of three leads though modelling of: (a) the likelihood of reactivation for all faults within and adjacent to, the leads and, (b) across-fault juxtaposition of bulk sandstone and shale intervals. The fault seal analysis was carried out using Badley Geoscience Pty Ltd's *TrapTester*TM software. Lastly, the study area extends from the Rosedale Fault System to the eastern Central Deep (Fig. 1).

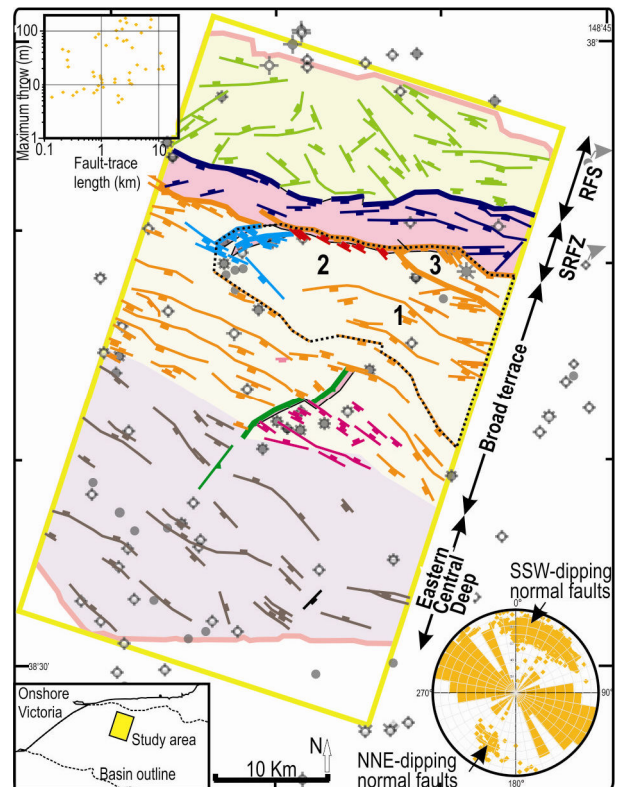


Figure 1. Location map-study area. Distribution of fault azimuth across the broad terrace (lower right) and associated fault-trace length and throw (upper left). Fault sub-provinces

and mode are differentiated by colour. Dashed line–area, incorporating leads 2 and 3 where the fault seal analysis was carried out. RFS–Rosedale Fault System; SRFZ–south Rosedale fault zone.

METHOD AND RESULTS

Seismic interpretation and depth conversion

A seismic interpretation of a 3-D cube was carried out in the time domain on a *GeoFrame*TM workstation using the *Geoquest*TM interpretation software. The interpretation incorporated log, well and age–depth data from 95 wells – 14 sequence boundaries were interpreted according to a new sequence–stratigraphic scheme, the latter enabling detailing of the structural history (Sayers, 2011). The variance attribute was extracted from the seismic volume and used to interpret fault planes in combination with seismic profiles (Fig. 2). The lower limit of fault throw delineation across the volume was estimated by determining the seismic resolution (EQ-1 and -2); for example, at a typical reservoir depth of 2.5 km, the limit of vertical and lateral separability is estimated at 12 and 480 m, respectively. See Brown (2004) for methodology and Sayers (2011) for results of the parent study. The upper bound of fault throw is ~ 200 m (Fig. 1).

Quarter wavelength = [depth + 6.3]207.4 m ($R^2 = 0.76$) EQ. 1
Fresnel Zone = depth/5.175 m ($R^2 = 0.9774$) EQ. 2

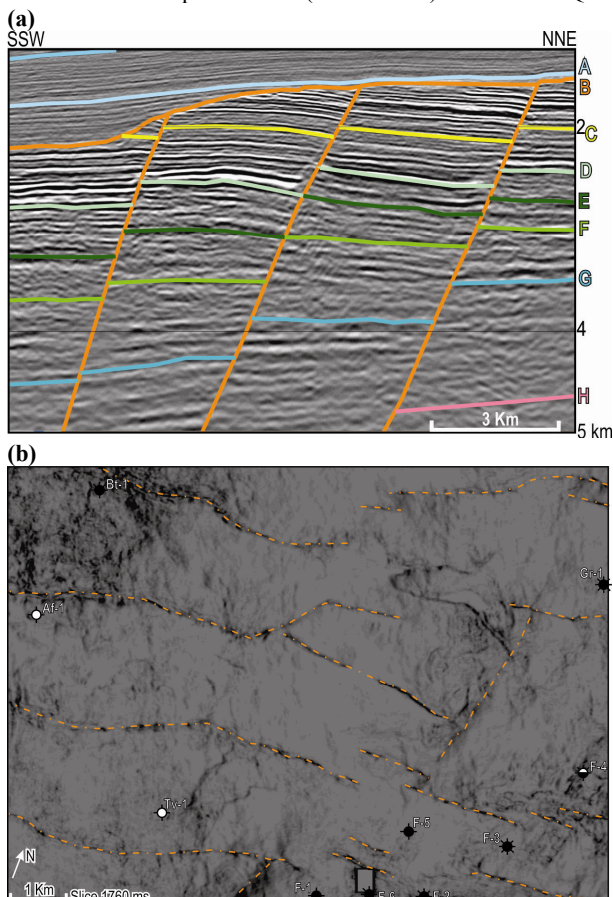


Figure 2. Typical fault offsets on the broad terrace delineated using (a) a seismic section and, (b) the variance attribute.

The depth–conversion method used a software program, initially developed by W. Seweryn for depth–converting 2-D seismic data (<http://users.chariot.net.au/~witek/t2d.htm>); it was enhanced to depth–convert a 3-D seismic cube. The depth–

conversion method used a multi–well, one TWT–depth function per well based on 57 sets of checkshots. A root mean square error of $\sim \pm 17$ m (at 1 Stdev) and ± 27 m (at 2 Stdev) was estimated at well locations. The depth error, whilst being large in an absolute sense, was deemed acceptable in a relative sense since the objective was to estimate reservoir–seal offsets across–fault, as opposed to depth prognoses of reservoir targets. See Sayers (2011) for further description.

Fault reactivation modelling

Fault reactivation is modelled by considering the increase in pore pressure (ΔP) required to reduce the effective stress sufficiently to cause shear, extensional shear or extensional failure on an intact/healed fault. In this regard, the rock strength ($C = 2$) and failure envelope (coefficient of friction = 0.75) adopted were estimated using a percentage breakout of lithologies as determined from log cutoffs: 81% sandstone, 10% shale and 9% other lithologies (Sayers, 2011). The parameters that follow form the input to modelling the ΔP for the 62 faults being considered (mostly ‘branched’ faults). A S_{Hmax} , S_{Hmin} and S_V of 42, 20 and 21 MPa/km, respectively, are used based on Nelson *et al.* (2006). A pore pressure of 10 MPa/km is used to calculate the effective stress. Also, the maximum shear stress direction is taken as $139^\circ N$ ($S_{Hmax\theta}$). The associated stress regime, according to Andersonian principles, is taken as borderline reverse–strike–slip.

The ΔP modelled for the ‘branched’ faults (Fig. 3a), indicate that NE–SW faults are least likely to reactivate (Fig. 3b); these trend at obtuse angles to $S_{Hmax\theta}$. This observation may also be part of the reason why the Flounder, Tuna and West Tuna Fields have petroleum accumulations (Figs 1 and 3b). When considering the ‘branched’ faults, the splays have a negative impact (or detrimental to trap integrity) for 32 % of branch–line cases considered, have positive impact for 26% and, the change being minimal for the remaining 42%. It was also demonstrated that the likelihood of reactivation can be low across portions of the elongated fault planes, some up to 12 km, where the strike also deviates from trend by up to $\pm 33^\circ$ (Fig. 3b).

Across–fault juxtaposition of reservoir–seal intervals

The parent study that assessed across–fault juxtaposition considered both the volume of shale and shale gouge ratio (V_{shale} , SGR; Sayers, 2011), the latter an estimate of shale smear across a fault plane. The SGR is then associated to the likelihood of fluid transmissivity; for example, a SGR in excess of 0.15–0.2 is normally taken as being indicative of non–transmissivity (Yielding, 1997). Both the V_{shale} and SGR are derived using the gamma–ray log and projected onto the fault plane. Modelling of the SGR indicates that portions of some fault planes can potentially retain hydrocarbon columns (Fig. 4), subject to shale smear being present.

A fault plane’s hydrocarbon retention capacity can be further modelled by deriving the ‘column height’ attribute using Badley Geoscience Ltd’s *TrapAnalyst*TM sub–program. Figure 5 shows that although the column height (estimated here based on the SGR) can be considerable, a fault trap’s leak point will be dependant on the fluid transmission cut–off as arbitrarily set from the SGR assigned to it. For the specific fault and lead considered here, the fault trap’s retention capacity is estimated to be ~ 10 % of its total column–height capacity. The modelling results portray why fault traps in the Halibut Subgroup and, in this part of the basin, are likely to be either unfilled or only partly filled.

Implications for petroleum exploration

Modelling across-fault juxtaposition of reservoir–seal intervals was found to be most sensitive to well control. Well control is fundamental in adequately projecting onto the fault plane the lithology, V_{shale} and SGR so as to estimate the sand-on-sand and sand-on-shale windows. Ultimately, the inherent limitation to the modelling resulting from inadequate well-control ultimately limits the prediction of fault-seal integrity. This is particularly the case in the study area where the sandstone-to-shale ratio is high. The implication would be that fault traps are more likely to have better across-fault seal potential in a downdip basinal position, closer to the depocentre and, where the sand-to-shale ratio decreases. Relative to the above, the impact of fault tips, ‘branched’ faults and presence of shale smear is secondary. Thus, the successful pooling of hydrocarbons in fault traps is problematic within the study area although possible, as has been demonstrated in the Flounder Field (ESSO, 1988). Other exceptions exist in the Golden Beach and Emperor Subgroups as have been demonstrated in the Kipper and Longtom Fields (Lanigan *et al.*, 2007; Sloan *et al.*, 1992).

CONCLUSIONS

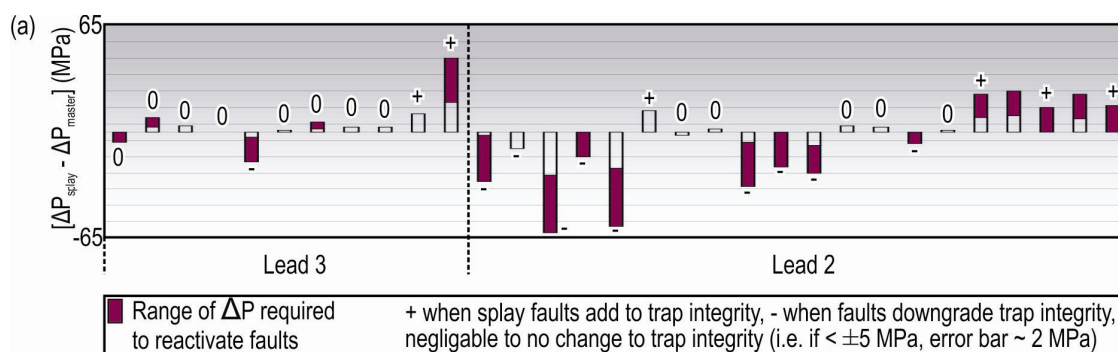
The likelihood of reactivation of faults in ‘branched’ fault traps is most sensitive to the strike of the faults relative to $S_{\text{Hmax}\theta}$. Any increase in pore pressure pushes a fault closer to the failure envelope (i.e. as demonstrated on a Mohr Circle); thereby, trap integrity is most robust where the ‘branched’ faults have the highest combined ΔP . The above study shows the potential reduction in ΔP when introducing splays – it follows that regional-based fault-reactivation estimates that do not incorporate splay faults (e.g. van Ruth *et al.*, 2006) have limited application with regards to fault-trap integrity. The parent study (Sayers, 2011) demonstrated that the sandstone percentage in the Halibut Subgroup and study area is of the order of 81%. Consequently, the high proportion of across-fault sand-on-sand windows and inconsistent shale smear precludes any significant hydrocarbon columns from being trapped against any significant length of any of the larger fault planes. This is the case whether a trap has ‘branched’ faults present or not. Fault traps, although known to hold hydrocarbons in the eastern Gippsland Basin, are not likely to be the main trap objective in the larger portion of the study area. There would be a higher likelihood of petroleum-bearing fault traps located closer to the depocentre in the eastern Central-Deep. Lastly, fault rock and zone damage information were unavailable to the project so that the estimate of cohesion and friction coefficient (used in the fault reactivation modelling) was based on lithology alone. Ultimately, ascertaining any breach-of-trap would also be contingent on sealing characteristics of any potential fault rock and/or aperture of any fault zone being modelled.

ACKNOWLEDGMENTS

I acknowledge the University of Adelaide, Geoscience Australia and the Cooperative Centre for Greenhouse Gas Technologies for supporting the research. I also thank Central Petroleum Ltd for allowing me to present at the ASEG.

REFERENCES

- Brown, A.R., 2004, Interpretation of three-dimensional seismic data: In Lorenz, J.C. and Schuster, G.T. (Eds), AAPG Memoir 42 SEG Investigations in Geophysics No 9 (6th edition), p541.
- ESSO, 1988, The Gippsland Basin–Petroleum in Australia–The First century: The APEA Journal, 28, 174-190.
- Etheridge, M.A., McQueen, H. and Lambeck, K., 1991, The role of intraplate stress in Tertiary deformation of the Australian continent and its margins: a key factor in petroleum trap formation: Exploration Geophysics, 22, 123-128.
- Lanigan, K.P., Bunn, G. and Rindschwentner, J., 2007, Longtom–confirmation of a new play in offshore Gippsland: The APPEA Journal, 47, 89–104.
- Maung, T.U., 1992, A regional synthesis of the offshore Gippsland Basin: Exploration Geophysics, 20(1–2), 313-323.
- Nelson, E.J., Hillis, R.R., Sandiford, M., Reynolds, S. and Mildren, S.D., 2006, Present-day state-of-stress of southeast australia: The APPEA Journal, 46, 283-305.
- Power, M.R., Hill, C.K. and Hoffman, N., 2003, Structural inheritance, stress rotation, overprinting and compressional reactivation in the Gippsland Basin–Tuna 3-D seismic dataset: The APPEA Journal, 43, 197-221.
- Sayers, J., 2011, Seismic interpretation of the eastern Gippsland Basin with application to fault seal analysis in carbon dioxide storage leads: Ph.D. Thesis, University of Adelaide.
- Sloan, M.W., Moore, P.S. and McCutcheon, 1992, Kipper—a unique oil and gas discovery, Gippsland Basin, Australia: The APEA Journal, 32, 1-8.
- van Ruth, P.J., Nelson, E.J. and Hillis, R.R., 2006, Fault reactivation potential during CO₂ injection in the Gippsland Basin, Australia: Exploration Geophysics, 37, 50-59.
- Yielding, G., Freeman, B. and Needham, D.T., 1997, Quantitative fault-seal prediction: AAPG Bulletin, 81, 897-917.



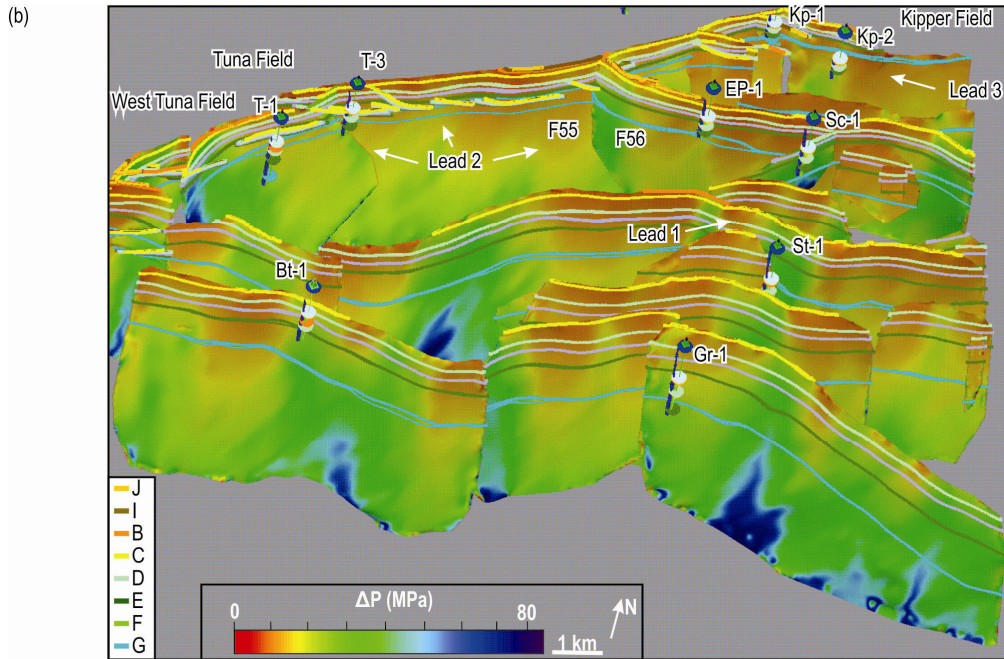


Figure 3. Modelled increase in pore pressure (ΔP) required to induce reactivation of 'branched' faults for the two leads considered. (a) Bar graph representation. (b) 3-D representation. See figure 1 for the location of faults and leads.

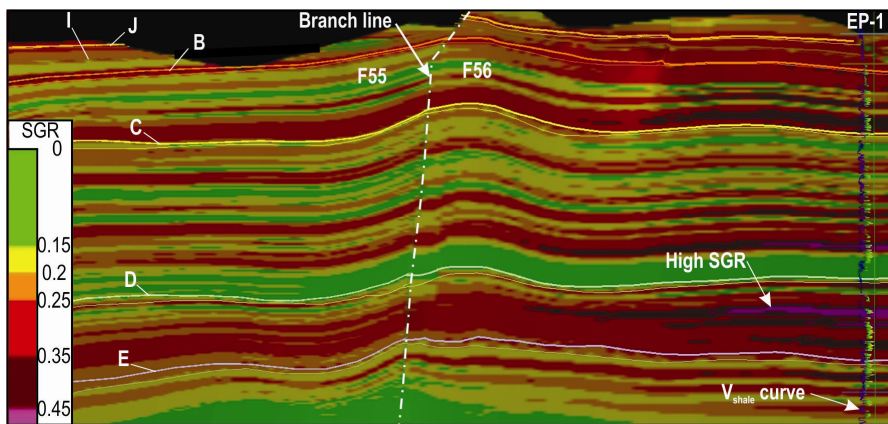


Figure 4. The shale gouge ratio (SGR) portrayed across two fault planes as projected from nearby wells and conforming to interpreted surfaces. A branch line for faults F55 and F56 is shown. See figures 1 and 3b for the location of faults.

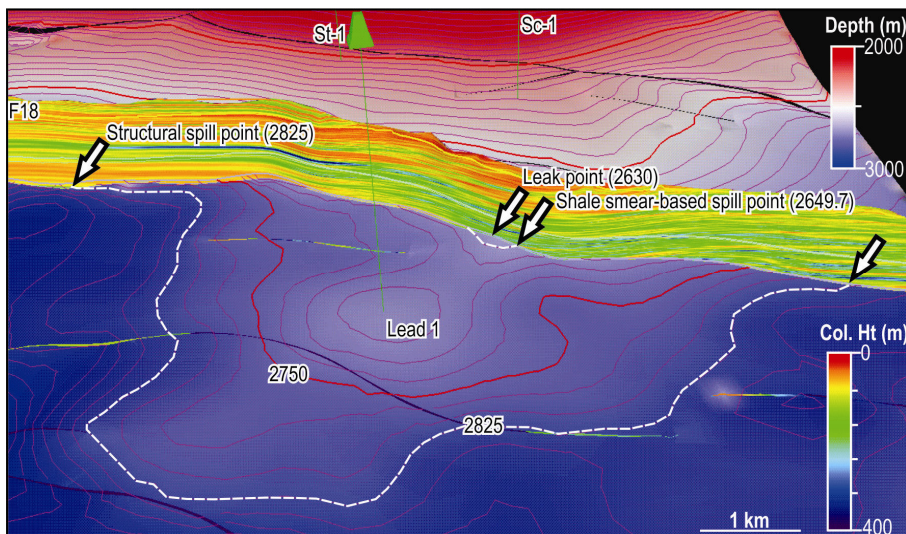


Figure 5. 3-D representation of a fault trap. The column height attribute is shown across the fault plane as well as the leak, structural and shale seal-based spill points. See figures 1 and 3b for the location of the lead. Col. – column.